Research article

Prediction of placenta accreta spectrum in patients with placenta previa using a clinical, US and MRI combined model: A retrospective study with external validation

Simone Maurea [a], Francesco Verde [a,b], Valeria Romeo [a], Arnaldo Stanzione [a,*],
Pier Paolo Mainenti [c], Giorgio Raia [a], Luigi Barbuto [b], Francesca Iacobellis [b],
Fabrizia Santangelo [g], Laura Sarno [d], Sonia Migliorini [d], Mario Petretta [e], Maria D'Armiento [a],
Gianfranco De Dominicis [f], Claudio Santangelo [g], Maurizio Guida [d], Luigia Romano [b],
Arturo Brunetti [a]

[a] *University of Naples "Federico II", Department of Advanced Biomedical Sciences, Naples, Italy*
[b] *Department of General and Emergency Radiology, "Antonio Cardarelli" Hospital, Naples, Italy*
[c] *Institute of Biostructures and Bioimaging of the National Council of Research (CNR), Naples, Italy*
[d] *University of Naples "Federico II", Department of Neuroscience, Reproductive and Dentistry Sciences, Naples, Italy*
[e] *IRCCS, Synlab SDN, Naples, Italy*
[f] *Department of Anatomical Pathology, "Antonio Cardarelli" Hospital, Antonio Cardarelli, Naples, Italy*
[g] *Department of Obstetrics and Gynecology, "Antonio Cardarelli" Hospital, Naples, Italy*

ARTICLE INFO

ABSTRACT

Purpose: To build and validate a predictive model of placental accreta spectrum (PAS) in patients with placenta previa (PP) combining clinical risk factors (CRF) with US and MRI signs.
Method: Our retrospective study included patients with PP from two institutions. All patients underwent US and MRI examinations for suspicion of PAS. CRF consisting of maternal age, cesarean section number, smoking and hypertension were retrieved. US and MRI signs suggestive of PAS were evaluated. Logistic regression analysis was performed to identify CRF and/or US and MRI signs associated with PAS considering histology as the reference standard. A nomogram was created using significant CRF and imaging signs at multivariate analysis, and its diagnostic accuracy was measured using the area under the binomial ROC curve (AUC), and the cut-off point was determined by Youden's J statistic.
Results: A total of 171 patients were enrolled from two institutions. Independent predictors of PAS included in the nomogram were: 1) smoking and number of previous CS among CRF; 2) loss of the retroplacental clear space at US; 3) intraplacental dark bands, focal interruption of the myometrial border and placental bulging at MRI. A PAS-prediction nomogram was built including these parameters and an optimal cut-off of 14.5 points was identified, showing the highest sensitivity (91%) and specificity (88%) with an AUC value of 0.95 (AUC of 0.80 in the external validation cohort).
Conclusion: A nomogram-based model combining CRF with US and MRI signs might help to predict PAS in PP patients, with MRI contributing more than US as imaging evaluation.

1. Introduction

Placenta accreta spectrum (PAS) is determined by the invasion of chorionic villi within the myometrial layer [1]. Depending on the depth of the penetration of placental villi i.e. decidua basalis of the myometrium, two types of PAS can be identified, namely placenta accreta or

increta, respectively [2]. Villi can also extend throughout the myometrium and going beyond it, a condition defined as placenta percreta [2]. The major risk factor of PAS is represented by the abnormal location of the placental tissue into the lower uterine segments, a condition where the placental edge is located within 2 cm of the internal os (low-lying placenta) or extends over the internal os (placenta previa – PP)[3,4]. The incidence of PAS is also increasing along with the number of cesarean sections (CS), since the uterine scar represents a defect of the myometrial wall placental villi can invade first [5]. Other patients' clinical features have been reported as related to the occurrence of PAS, such as smoking during pregnancy, maternal age and arterial hypertension [3]. During pregnancy, the early identification of PAS in high-risk patients is important to establish the appropriate patient management during the delivery, since a non-detachment of the placenta from the myometrium can occur determining even fatal hemorrhage [6]; indeed, patients with PAS often require the prophylactic embolization of uterine artery as well as blood transfusion [7].

Along with clinical risk factors (CRF), imaging is also helpful for the early identification of PAS; in this setting, ultrasound (US) is the first-level imaging modality, with a reported good accuracy using specific findings suggestive of PAS [5], even if its overall accuracy is still debated [8]. To overcome well-known limitations of US such as operator dependence and cases of posterior placental location, magnetic resonance imaging (MRI) has been proposed as a second-level imaging modality, especially when US is not conclusive [7,9]. The increasing use of MRI goes together with the improved ability of radiologists in identifying specific MRI signs suspected for PAS as well as with the identification of systematic methods to diagnose PAS, the most effective consisting of the presence of at least two abnormal MRI signs [10–13]. An MRI-based predictive model has been recently proposed to predict patients' clinical outcomes using MRI signs [14]. What emerges from the current literature is that a definitive method to predict PAS early has not been established yet, with combined approaches appearing as the most promising way to maximize PAS prediction accuracy. In this regard, clinical-US integrated indexes have been recently suggested as models for improving US prediction of PAS [15,16] as well as integrated imaging methods using CRF, US and MR signs to predict PAS have been recently investigated [13,17–20]. Furthermore, artificial intelligence techniques to predict PAS in patients with PP have been recently proposed as potential additional diagnostic tools [21–25].

Considering the overall contribution that either clinical risk factors as well as US and MRI signs may give to the identification of PAS, the aim of this study was to combine such data to build and validate a clinical-imaging model to predict PAS in patients with PP.

2. Methods

2.1. Patient population

Patient population consisted of two groups of PP patients from different institutions of which the first was the training group (Institution 1) while the second was the external validation group (Institution 2). In both groups, consecutive pregnant patients who underwent US and MRI examinations for suspicion of PAS were retrospectively selected. The following clinical data, considered as CRF for PAS, were retrieved from medical records and collected for each patient: maternal age (years), smoking during pregnancy (yes/not), number of previous CS and arterial hypertension defined as > 140/90 mmHg (yes/not) [26]. In both groups, inclusion criteria were: >18-year-old patients with PP; patients in which US and MRI examinations were performed within the same week; patients with available histological proof of PAS after CS or hysterectomy. We excluded patients for whom US or MRI images were not retrieved or incomplete for the retrospective evaluation as well as MR examinations significantly affected by mother/fetal motion artifacts; patients with incomplete clinical data were also excluded. The study was approved by our institutional review board, and written informed consent was obtained in all patients.

2.2. US acquisition

Training Group. Transabdominal and transvaginal US examinations were performed by an obstetrician trained in placenta sonographic assessment, using a GE Healthcare Voluson E8 (GE Healtcare, Milwaukee, WI) US machine with a 5 MHz convex probe and a 7 MHz transvaginal convex probe. Placental location, internal structure as well as the relationship with neighbouring organs were first evaluated on B-mode examination. Color-Doppler US examination was performed to assess blood flow at the level of suspected placental lacunae identified at B-mode evaluation.

Validation External Group. Ultrasound studies were conducted by a highly experienced obstetrician employing a GE Healthcare Voluson S10 (GE Healtcare, Milwaukee, WI) US device equipped with a 5 MHz convex probe for the transabdominal examination and a 9 MHz curved transvaginal array probe. In detail, morphological features were first evaluated through B-mode examination such as placental location, internal structure, and its relationship with adjacent organs; successively, the color-Doppler US imaging was performed to evaluate blood flow, specifically at the suspected placental lacunae identified during the B-mode evaluation.

2.3. MR acquisition protocols

Training Group. MRI was performed using a 1.5 T scanner (Gyroscan, Intera, Philips, Best, The Netherlands) with a phased-array body coil. The following MR sequences were acquired: Single-shot Turbo-Spin-Echo (TSE) T2-weighted sequence (FOV 405 × 321 mm, matrix: 232x164, slice thickness 5–6 mm, number of slice 40, Flip angle: 90°, GAP 1, TR/TE = 381/80 ms) on axial, sagittal and coronal planes; breath-holding was requested to minimize respiratory motion artefact; and Thrive Spectral Attenuated Inversion Recovery (SPAIR) T1-weighted sequence (FOV: 395x280x340 mm, matrix: 192x192, slice thickness 4 mm, number of slice 60, Flip angle: 10°, GAP 2, TR/TE = 3.6/1.7 ms). No contrast agent injection was performed. MRI duration time was around 20 min.

Validation External Group. MR was performed using a 1.5 T scanner (Signa Explorer, GE Healthcare, Milwaukee, Wisconsin, USA) with a phased-array body coil. The following MR sequences were acquired: Single-shot Fast-Spin-Echo T2-weighted sequence (FOV 400 × 320 mm, matrix: 320x216, slice thickness 5–6 mm, number of slice 35–40, Flip angle: 120°, GAP 1, TR/TE = 800/85 ms) on axial, sagittal and coronal planes; breath-holding (15 sec.) was requested to minimize respiratory motion artefact; and Fat-Saturated Spoiled Gradient-Recalled Echo T1-weighted sequence (FOV: 400x320mm, matrix: 256x192, slice thickness 3 mm, number of slice 70, Flip angle: 10°, GAP 2, TR/TE = 4.3/1.6 ms). No contrast agent was used. MRI duration time was around 20 min.

2.4. Image analysis

The presence of the following US findings suggestive of PAS [13,17,18,23] was assessed by two obstetricians trained in placenta sonographic assessment in consensus, blinded to clinical data and histological diagnosis: 1) Abnormal placental lacunae (PL), defined as numerous, large and irregular lacunae hypervascularized at color-Doppler evaluation (Finberg grade 3); 2) myometrial thinning (MT), < 1 mm or undetectable; 3) placental bulge (PB), consisting of a protrusion of the uterine serosa; 4) loss of the retroplacental clear space (LRCS); 5) focal exophytic mass (FEM), defined as the presence of placental tissue extending beyond the uterine serosa; and 6) bladder wall interruption (BWI), defined as loss or interruption of the hyperechoic band between the uterine serosa and the bladder wall. In case of disagreement, a third obstetrician with 32 years of experience was consulted. Similarly, MR images were analyzed in consensus by two radiologists with fifteen and

eighteen years of experience in genitourinary MRI, respectively, blinded to clinical history and pathological diagnosis. The presence of the following MR signs suggestive of PAS was assessed, as previously reported [16,26]: 1) intraplacental dark bands (IDB), consisting of areas of low signal intensity on T2-weighted images; 2) focal interruption of myometrial border (FIMB); 3) abnormal vascularity (AV), consisting of tortuous and enlarged flow voids on T2-weighted sequence deep within placental tissue and/or at the level of the uterine serosa; 4) placental bulging (PB) as loss of normal "pear shape" of the uterus; 5) tenting of the bladder (TB), meaning a bladder with pinched and stretched walls; and 6) direct visualization of adjacent tissues invasion (ATI). In case of disagreement, a third radiologist with 22 years of experience was consulted.

2.5. Statistical analysis

The Kolmogorov-Smirnov test was used to determine whether continuous clinical variables (maternal age, gestational age) were normally distributed. In the absence of normal distribution, the differences between the training and validation groups were assessed using the Mann-Whitney *U* test. Categorical variables (smoking, hypertension, number of previous CS, hysterectomy, presence of PAS), expressed as count and percentages, and differences between the two groups were evaluated using the Fisher exact test. Logistic regression analysis was performed on data from the training group to identify CRF and/or US and/or MRI signs associated with PAS, considering histology as the standard of reference. Only CRF and imaging signs significant at univariate analysis were considered for multivariable analysis. A nomogram was created using significant CRF and imaging signs at multivariate analysis to provide an intuitive and quantitative tool to predict the probability of PAS [27]; diagnostic accuracy was measured using the area under the binomial ROC curve (AUC) and the cut-off point, optimally classifying patients in a binary prediction problem, was determined by Youden's J statistic [28]. Finally, the external validation of the nomogram built on the training group data was performed in the validation group. Statistical analysis was made using Stata 15.1 software (StataCorp, College Station, TX). A two-sided p-value < 0.05 was considered significant.

3. Results

The demographic characteristics of the two groups of patients are illustrated in Table 1. Patients of the training group consisted of one-hundred-twenty patients with PP (Institution 1), while patients of the external validation group consisted of fifty-one patients with PP (Institution 2). In the training group, 34 (28%) patients had PAS confirmed by histological examination, while the remaining 86 (72%) patients were free of PAS. In the validation group, 13 (25%) patients had PAS confirmed by histological examination, while the remaining 38 (75%) patients were free of PAS. Univariate analysis showed significant only the smoking and the number of previous CS as CRF, all but one (focal exophytic mass) US imaging signs as well as all but two (tenting of the bladder and direct visualization of adjacent tissues invasion) MRI signs (Table 2); multivariate analysis confirmed as significant only the smoking and the number of previous CS as CRF, LRCS by US, IDB, FIMB and PB by MRI (Table 3). Successively, a nomogram was created including all significant CRF and imaging signs associating a score to each variable (Fig. 1); the individual point scores of CRF, US and MRI signs used for building the nomogram are reported in Table 4; in particular, among imaging signs, the highest score was given to each MRI variable with PB associated with the highest score (10 points), while the lowest score was by the LRCS on the US (4.6 points). To discriminate between positive and negative cases in terms of the probability of PAS, a cut-off of 14.5 points was identified on the nomogram, showing the highest sensitivity (91%) and specificity (88%) with an AUC value of 0.95 (Fig. 2). The integrated clinical-imaging model underlying the nomogram used to predict PAS was validated in patients of Group 2 showing an AUC value of 0.80 (Fig. 3). Examples of two patients from the study cohort showing both US and MRI corresponding images as well as the final nomogram scoring are illustrated in Figs. 4 and 5.

4. Discussion

The early identification of PAS in high-risk patients is fundamental to conduct the appropriate patient management during the delivery. In this regard, several CRF of PAS have been identified such as maternal age, multiparity, previous uterine surgery as well as previous CS [7]; recently, smoking during pregnancy and arterial hypertension have been identified as additional risk factors of PAS [3]. However, the most

Table 1
Clinical characteristics of patients in the groups of the two Institutions.

	Institution 1, train (n = 120)	Institution 2, validation (n = 51)	*p value*
Maternal Age, years (median, IQR)	34 (31–37)	35 (32–38)	0.285
GA (weeks) at US and MRI (median, IQR)	35 (33–37)	33 (31–34)	< 0.001*
Smoking (count, percentages)	27/120 (23%)	19/51 (37%)	0.059
Hypertension (count, percentages)	4/120 (3%)	0/51 (0%)	0.319
Previous CS (count, percentages)			
• 0	27/120 (23%)	20/51 (39%)	0.039*
• 1	53/120 (44%)	18/51 (35%)	0.312
• 2	29/120 (24%)	7/51 (14%)	0.153
• 3	7/120 (6%)	4/51 (8%)	0.735
• 4	4/120 (3%)	2/51 (4%)	0.999
Hysterectomy (count, percentages)	45/120 (38%)	19/51 (37%)	0.156
PAS Abnormality (count, percentages)	34/120 (28%)	13/51 (25%)	0.852

IQR = interquartile range, GA = gestational age, CS = cesarean section.

Table 2
Results of the univariable logistic analysis for CRF as well as US and MRI signs.

Variable		P value
CRF	Age	0.2541
	Number of CS	**0.000***
	Smoking	**0.015***
	Arterial hypertension	0.576
US	PL	**0.000***
	MT	**0.000***
	PB	**0.004**
	LRCS	**0.000***
	FEM	0.318
	BWI	**0.000**
MRI	IDB	**0.000***
	FIMB	**0.000***
	AV	**0.000***
	PB	**0.002**
	TB	0.079
	ATI	1.000

Note: CRF = clinical risk factors; US = ultrasound; MRI = magnetic resonance imaging; CS = cesarean section; PL = abnormal placental lacunae; MT = myometrial thinning < 1 mm; PB = Placental bulge; LRCS = Loss of the retroplacental clear space; FEM = Focal exophytic mass; BWI = Bladder wall interruption; IDB = Intraplacental bark bands; FIMB = Focal interruption of myometrial border; AV = abnormal vascularity; PB = uterine bulging; TB = tenting of the bladder; ATI = Adjacent tissue invasion. *significant p value < 0.05.

Table 3
Results of the multivariable logistic analysis for CRF as well as US and MRI signs significant at the univariable logistic analysis.

Variable		P value
CRF	Number of CS	**0.000***
	Smoking	**0.05***
US	PL	ns
	MT	ns
	PB	ns
	LRCS	**0.025***
	BWI	ns
MRI	IDB	**0.000***
	FIMB	**0.029***
	AV	ns
	PB	**0.005**

Note: CRF = clinical risk factors; US = ultrasound; MRI = magnetic resonance imaging; CS = cesarean section; PL = abnormal placental lacunae; MT = myometrial thinning < 1 mm; PB = Placental bulge; LRCS = Loss of the retroplacental clear space; FEM = Focal exophytic mass; BWI = Bladder wall interruption; IDB = Intraplacental bark bands; FIMB = Focal interruption of myometrial border; AV = abnormal vascularity; PB = placental bulging; TB = tenting of the bladder; ATI = Adjacent tissue invasion. *significant p value < 0.05.

commonly reported risk factor consists of the combination of previous cesarean delivery and PP [29]. US is considered the first-line imaging modality for the diagnosis of PAS, while MRI may be useful in assessing the pelvic extension of placenta percreta or anatomic areas difficult to evaluate on US, as shown by the recommendations of FIGO consensus guidelines on PAS disorders for prenatal diagnosis and screening [7]. Recently, a comparative guidelines study showed the need for new

prospective controlled cohort investigations and randomised controlled trials to compare the efficacy of different diagnostic techniques as well as therapeutic approaches in patients with PP [30]; in particular, it was stated that MRI is not essential for making a prenatal diagnosis of suspected PAS and, therefore, it is not the preferred primary imaging modality for the evaluation of women at risk of PAS; moreover, its use is limited by high cost and the availability of radiology experts for imaging assessment [31]. Similarly, a recent review study demonstrated that there was no general agreement regarding the indication of MRI in patients with PP to predict PAS [32]. Therefore, considering the overall contribution that either CRF or US and MRI imaging findings may give to the diagnosis of PAS, in this study we integrated such data to realize a clinical-imaging model to predict PAS in high-risk patients. In this

Table 4
The individual score of significant CRF, US and MRI imaging signs significant at multivariate analysis and used for building the nomogram.

| Variable			Scores (points)
CRF	Number of cesarean sections	1	1.5
		2	2.9
		3	4.4
		4	5.9
	Smoking		5
US signs	Loss of the retroplacental clear space		4.6
MRI signs	Intraplacental dark bands		8.7
	Focal interruption of the myometrial border		4.8
	Placental bulging		10

Note: CRF = clinical risk factors; US = ultrasound; MRI = magnetic resonance imaging.
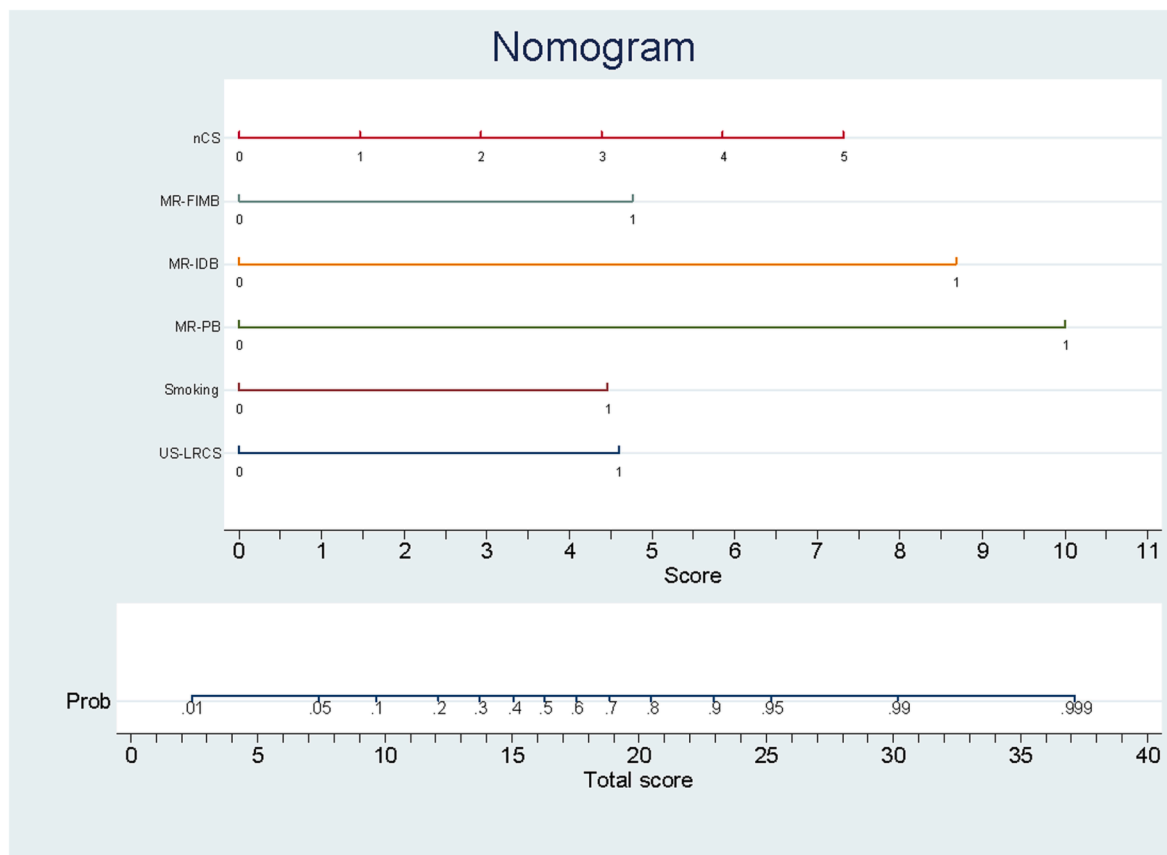
Fig. 1. Nomogram including CRF, US and MRI signs statistically significant at multivariable analysis; the presence of CRF as well as of US and MRI signs is associated to a score (see Table 4 for individual scoring); the total score is related to the probability of PAS. **Note:** nCS = number of previous cesarean sections; MR-FIMB = Focal interruption of myometrial border on MRI; MR-IDB = Intraplacental bark bands on MRI; MR-PB = Placental bulging; US-LRCS = Loss of the retroplacental clear space on US.
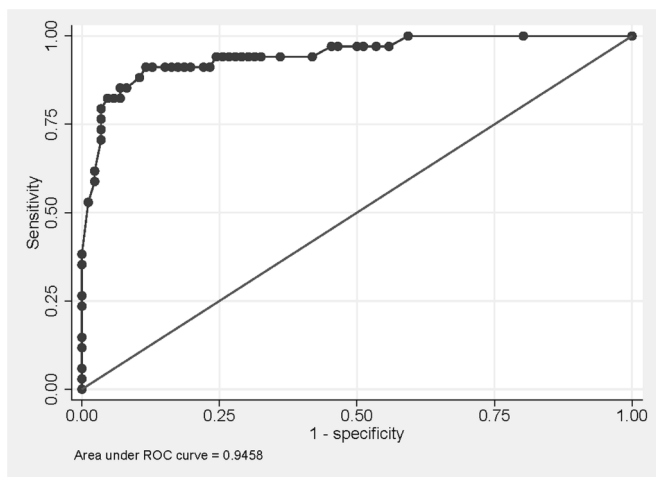
Fig. 2. ROC curve showing the accuracy of the nomogram obtained combining CRF, US and MRI signs in terms of probability of PAS in the training group (Group 1).
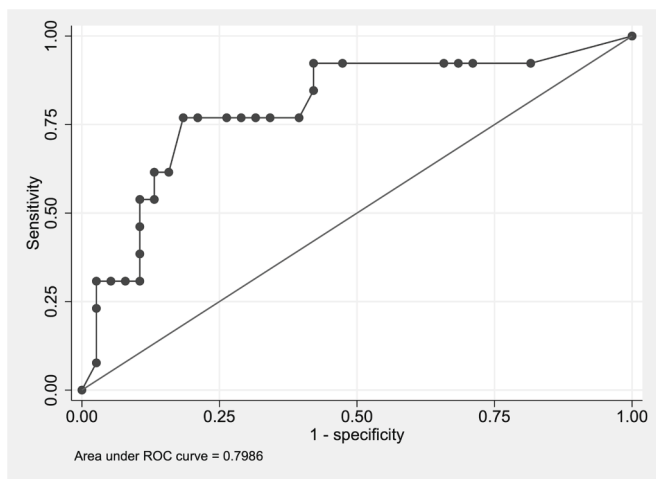

Fig. 3. ROC curve showing the accuracy of the nomogram obtained in the training group combining CRF, US and MRI signs in terms of probability of PAS in the external validation group (Group 2).

regard, in the training group all patients had PP, as well as the majority (78%) of patients, had at least one previous cesarean section [29]; moreover, an additional significant CRF, represented by smoking during pregnancy, was found to further characterize our patients as high-risk

population. To translate our results into clinical practice, in which CRF are routinely collected and US examinations always performed, we integrated significant CRF as well as US and MRI imaging signs to realize a model to be clinically used in high-risk patients to predict PAS.

Our results in the training group suggested that the combination of CRF with US and MRI signs may be effective in predicting PAS in patients with PP with an AUC value of 0.95. In particular, the model comprehended the variable association of two CRF, such as the occurrence of previous cesarean sections and the habit of smoking, with the presence of LRCS on US as well as of IDB, PB and FIMB on MRI. When we tested the model in the external validation group for the same purpose the AUC value was 0.80, suggesting an effective role of the combination of CRF with imaging signs. In agreement with previous findings [13], the main predictive contribution derives from MRI with the presence of three imaging signs in the model of which PB was associated with the highest score (10 points), followed by the presence of IDB (8.7 points) and FIMB (4.8 points). A positive clinical history of previous CS (score from 1.5 to 5.9 points) as well as the habit of smoking were also present in the model, as well as the presence of LRCS on US (4.6 points). Several studies assessed and compared the diagnostic accuracy of US and MRI to detect PAS [33]. Although conflicting results are reported regarding the comparison between the two modalities [34], it can be affirmed that both provide good and comparable accuracy values [11,33,35,36]. Similarly, different scoring systems, including clinical data and US signs [15,16] as well as US and MRI signs [13,17] have been proposed. Considering the even more frequent use of MRI in cases suspected for PAS and the routine assessment of clinical and US data, it is reasonable to propose a predictive model combining the most relevant CRF and imaging signs to predict PAS in patients with PP. Our results are in line with the current literature in which the number of previous CS is reported as a well-recognized risk factor [3,29,37]. Smoking during pregnancy was also found as a CRF for PAS; specifically, a case-control study revealed that women who smoked had a twofold increase in the risk of abruption (relative risk = 2.05, 95% confidence interval (CI) 1.75–2.40) in comparison with nonsmokers [38]. Likewise, LRCS is reported as a feature of great sensitivity using US [39–41]. Regarding MRI signs, our results are in agreement with previous MRI studies reporting IDB, FIMB and PB as reliable signs to identify PAS [11,42–44].

As compared to the formerly proposed predictive models combining clinical data with US signs, a number of previous CS and PL were present in all cases. On the other hand, LRCS and MT have been alternatively included in the study of Marsoosi [16] and Rac [15], respectively. With regard to the combined US-MRI severity score reported by Knight et al, four US signs and six MRI signs were considered [17]. Of note, most of them were also included in our scoring system, which are LRCS among US signs as well as IDB, FIMB and PB among MRI signs. Moreover, a combination of CRF, US and MRI findings has been recently proposed using previous CS, surgical abortion and/or other uterine surgeries as
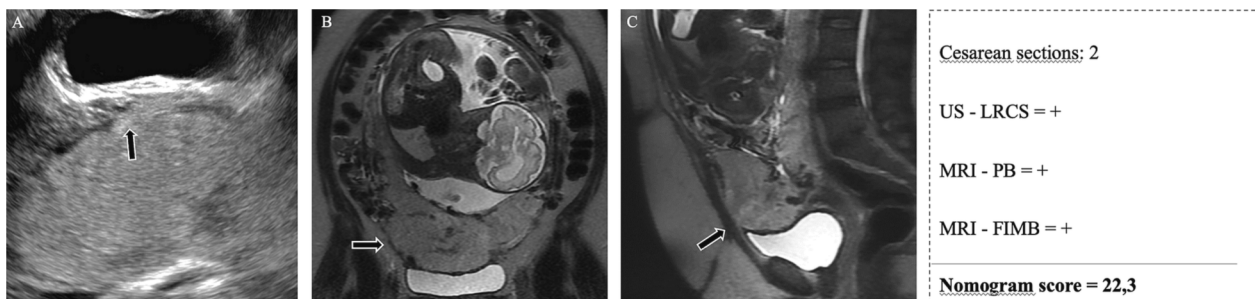
Fig. 4. Representative case of a 33-year-old woman at 32 gestation weeks with placenta previa. She had two previous cesarean sections and no history of smoking habits. At ultrasound (US) examination (A), the loss of the retroplacental clear space (LRCS) sign was identified (arrow). T2-weighted magnetic resonance images (MRI) demonstrated the presence of the placental bulging (B, coronal view) and focal interruption of myometrial border (C, sagittal view) signs. Based on the integrated clinical-imaging model, the nomogram score was 22,3, highly predictive of placenta accreta spectrum (PAS) disorders. The histological evaluation confirmed the diagnosis of PAS.
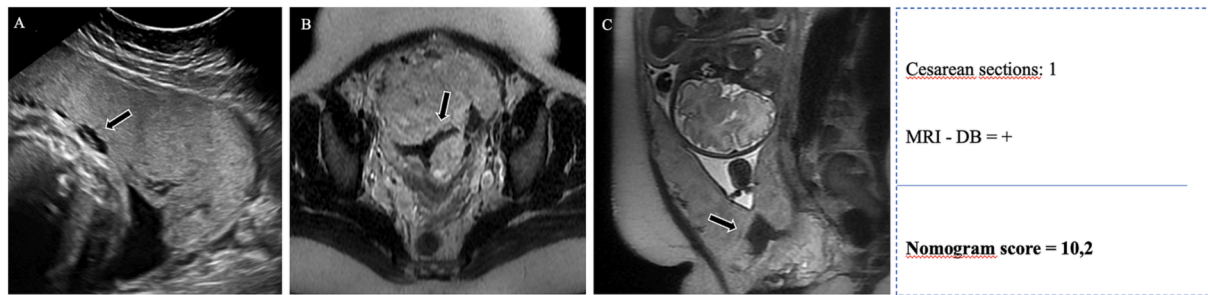
Fig. 5. Representative case of a 25-year-old woman at 35 gestation weeks with placenta previa. She had one previous cesarean section and no history of smoking habits. At ultrasound (US) examination (A), only abnormal placental lacunae were identified (arrow). T2-weighted magnetic resonance images (MRI) demonstrated the presence of intraplacental dark bands (DB) as shown on the axial (B) and sagittal (C) scans. Based on the integrated clinical-imaging model, the nomogram score was 10.2, not predictive of placenta accreta spectrum (PAS) disorders. The histological evaluation revealed a normal placenta.

well as US signs (grade of placental lacunae, loss of clear zone, turbulent blood flow and irregular signs) and MRI suspicion of adherent placenta [18]. Therefore, since the early diagnosis of PAS in patients with PP still remains a challenge in the clinical practice, the possibility of using a predictive clinical-imaging model integrating CRF as well as US and MRI signs could be helpful for patient management. In our study we identified a cut-off value of 14.5 points as total score to discriminate between positive and negative cases in terms of probability of PAS showing the highest sensitivity (91%) and specificity (88%) with an AUC value of 0.95. In this regard, Li et al. proposed an MRI nomogram for predicting invasive forms of PAS with comparable accuracy between internal and external validation groups [19]. Similarly, Pain et al. reported in their study an integrated US and MRI nomogram comparing placenta accretea/increta versus placenta percreta with good accuracy [20]. Recently, Hu et al. and Peng et al. described a novel model with a clinical-radiomic nomogram or with a deep-learning approach to predict PAS using MRI, respectively [24,25]. These studies support the integrated role of clinical and imaging findings to predict PAS in patients with PP; thus, a multi-disciplinary clinical-imaging evaluation of patients with PP is the optimal key to manage such patients. The Society of Abdominal Radiology (SAR) and the European Society of Urogenital Radiology (ESUR) joint consensus statement recommended that no single imaging sign is diagnostic for PAS, but the presence of multiple imaging signs by US and MRI in a clinical context of high risk increases the likelihood of underlying PAS [45]. Therefore, standardized combined clinical-imaging models might be helpful for this purpose.

Limitations of our study are firstly related to its retrospective design, with an intrinsic risk of selection bias. Secondly, the limited cases of placenta percreta could have reduced the relevance of specific MRI signs such as TB and ATI. Regarding the importance of MRI signs, it has been found that the diagnostic accuracy of MRI for PAS detection is influenced by the experience of radiologists [31,46,47] [;]. Given the expertise and sub-specialization of the radiologists working in consensus for this study, the nomogram performance might not be reliable if MRI readings are performed by less experienced or generalist radiologist. Thirdly, while the training and validation groups did not significantly differ in terms of PAS incidence in PP patients, the value was relatively higher than what was previously estimated [48]]. Allowing for a recognized degree of heterogeneity, this issue could still limit the generalizability of our findings. Finally, recent imaging guidelines recommend that MRI is performed at 28–32 weeks of GA for optimal diagnostic performance [49] even though GA was higher in our population at the date of MRI, the results on MRI signs diagnostic significance are encouraging and the utility of the imaging modality does not appear negatively affected.

In conclusion, our integrated clinical-imaging model combining CRF as well as US and MRI signs may be effective in predicting PAS in patients with PP and, thus, useful in the clinical practice to improve the detection of placental disorders; in particular, MRI contributed to the model more than US with three imaging signs compared to only one US sign suggesting a fundamental role of MRI. Additional prospective studies in different patient populations are needed to confirm the accuracy of our model in predicting PAS with the main role of MRI.

CRediT authorship contribution statement

Simone Maurea: Writing – original draft, Project administration, Methodology, Investigation, Formal analysis, Data curation, Conceptualization. **Francesco Verde:** Investigation, Formal analysis, Data curation. **Valeria Romeo:** Writing – review & editing, Validation, Supervision. **Arnaldo Stanzione:** . **Pier Paolo Mainenti:** . **Giorgio Raia:** Investigation, Data curation. **Luigi Barbuto:** Supervision, Project administration. **Francesca Iacobellis:** Investigation, Formal analysis, Data curation. **Fabrizia Santangelo:** Methodology, Investigation, Data curation. **Laura Sarno:** Methodology, Investigation, Formal analysis, Data curation. **Sonia Migliorini:** Formal analysis, Data curation. **Mario Petretta:** Formal analysis, Data curation. **Maria D'Armiento:** Formal analysis, Data curation. **Gianfranco De Dominicis:** Investigation, Data curation. **Claudio Santangelo:** Investigation, Data curation. **Maurizio Guida:** Investigation, Data curation. **Luigia Romano:** Supervision, Project administration. **Arturo Brunetti:** Supervision, Project administration, Conceptualization.

Declaration of Competing Interest

The authors declare that they have no known competing financial interests or personal relationships that could have appeared to influence the work reported in this paper.

Acknowledgments

References

[1] R.M. Silver, K.D. Barbour, Placenta Accreta Spectrum. Accreta, Increta, and Percreta., Obstet. Gynecol. Clin. North Am. (2015). https://doi.org/10.1016/j.ogc.2015.01.014.

[2] A.G. Cahill, R. Beigi, R.P. Heine, R.M. Silver, J.R. Wax, Placenta Accreta Spectrum, Am. J. Obstet. Gynecol. 219 (2018) B2–B16, https://doi.org/10.1016/j.ajog.2018.09.042.

[3] D.A. Carusi, The placenta accreta spectrum: Epidemiology and risk factors, Clin. Obstet. Gynecol. 61 (2018) 733–742, https://doi.org/10.1097/GRF.0000000000000391.

[4] V. Jain, H. Bos, E. Bujold, G. No, 402: Diagnosis and Management of Placenta Previa, J. Obstet. Gynaecol. Canada. 42 (2020) 906–917.e1, https://doi.org/10.1016/j.jogc.2019.07.019.

[5] E. Jauniaux, S. Collins, G.J. Burton, Placenta accreta spectrum: pathophysiology and evidence-based anatomy for prenatal ultrasound imaging, Am. J. Obstet. Gynecol. (2018), https://doi.org/10.1016/j.ajog.2017.05.067.

[6] J.R. Leyendecker, M. DuBose, K. Hosseinzadeh, R. Stone, J. Gianini, D.D. Childs, A. N. Snow, H. Mertz, MRI of Pregnancy-Related Issues: Abnormal Placentation, Am. J. Roentgenol. 198 (2012) 311–320, https://doi.org/10.2214/AJR.11.7957.

[7] E. Jauniaux, A. Bhide, A. Kennedy, P. Woodward, C. Hubinont, S. Collins, G. Duncombe, P. Klaritsch, F. Chantraine, J. Kingdom, L. Grønbeck, K. Rull, B. Nigatu, M. Tikkanen, L. Sentilhes, T. Asatiani, W.C. Leung, T. Alhaidari, D. Brennan, E. Kondoh, J.I. Yang, M. Seoud, R. Jegasothy, S. Espino y Sosa, B. Jacod, F. D'Antonio, N. Shah, D. Bomba-Opon, D. Ayres-de-Campos, K. Jeremic, T.L. Kok, P. Soma-Pillay, N. Tul Mandić, P. Lindqvist, T.B. Arnadottir, I. Hoesli, U. Jaisamrarn, A. Al Mulla, S. Robson, R. Cortez, FIGO consensus guidelines on placenta accreta spectrum disorders: Prenatal diagnosis and screening, Int. J. Gynecol. Obstet. (2018), https://doi.org/10.1002/ijgo.12408.

[8] Z.S. Bowman, A.G. Eller, A.M. Kennedy, D.S. Richards, T.C. Winter, P. J. Woodward, R.M. Silver, Accuracy of ultrasound for the prediction of placenta accreta, Am. J. Obstet. Gynecol. 211 (177) (2014) e1–177.e7, https://doi.org/10.1016/j.ajog.2014.03.029.

[9] B. Varghese, N. Singh, R. George, S. Gilvaz, Magnetic resonance imaging of placenta accreta, Indian J. Radiol. Imaging. 23 (2013) 379, https://doi.org/10.4103/0971-3026.125592.

[10] A.L. Valentini, B. Gui, V. Ninivaggi, M. Miccò, M. Giuliani, L. Russo, M.G. Marini, M. Tintoni, A.F. Cavaliere, L. Bonomo, The morbidly adherent placenta: When and what association of signs can improve MRI diagnosis? our experience, Diagnostic Interv. Radiol. 23 (2017) 180–186, https://doi.org/10.5152/dir.2017.16275.

[11] S. Maurea, V. Romeo, P.P. Mainenti, M.I. Ginocchio, G. Frauenfelder, F. Verde, R. Liuzzi, M. D'Armiento, L. Sarno, M. Morlando, M. Petretta, P. Martinelli, A. Brunetti, Diagnostic accuracy of magnetic resonance imaging in assessing placental adhesion disorder in patients with placenta previa: Correlation with histological findings, Eur. J. Radiol. (2018), https://doi.org/10.1016/j.ejrad.2018.07.014.

[12] P.J. Woodward, A. Kennedy, B.D. Einerson, Is There a Role for MRI in the Management of Placenta Accreta Spectrum? Curr. Obstet. Gynecol. Rep. 8 (2019) 64–70, https://doi.org/10.1007/s13669-019-00266-9.

[13] V. Romeo, L. Sarno, A. Volpe, M.I. Ginocchio, R. Esposito, P.P. Mainenti, M. Petretta, R. Liuzzi, M. D'Armiento, P. Martinelli, A. Brunetti, S. Maurea, US and MR imaging findings to detect placental adhesion spectrum (PAS) in patients with placenta previa: a comparative systematic study, Abdom. Radiol. (2019), https://doi.org/10.1007/s00261-019-02185-y.

[14] A. Delli Pizzi, A. Tavoletta, R. Narciso, D. Mastrodicasa, S. Trebeschi, C. Celentano, J. Mastracchio, R. Cianci, B. Seccia, L. Marrone, M. Liberati, A.R. Cotroneo, M. Caulo, R. Basilico, Prenatal planning of placenta previa: diagnostic accuracy of a novel MRI-based prediction model for placenta accreta spectrum (PAS) and clinical outcome, Abdom. Radiol. 44 (2019) 1873–1882, https://doi.org/10.1007/s00261-018-1882-8.

[15] M.W.F. Rac, J.S. Dashe, C.E. Wells, E. Moschos, D.D. McIntire, D.M. Twickler, Ultrasound predictors of placental invasion: the Placenta Accreta Index, Am. J. Obstet. Gynecol. 212 (343) (2015) e1–343.e7, https://doi.org/10.1016/j.ajog.2014.10.022.

[16] V. Marsoosi, F. Ghotbizadeh, N. Hashemi, B. Molaei, Development of a scoring system for prediction of placenta accreta and determine the accuracy of its results, J. Matern. Neonatal Med. 33 (2020) 1824–1830, https://doi.org/10.1080/14767058.2018.1531119.

[17] J.C. Knight, S. Lehnert, A.L. Shanks, L. Atasi, L.R. Delaney, M.B. Marine, S. A. Ibrahim, B.P. Brown, A comprehensive severity score for the morbidly adherent placenta: combining ultrasound and magnetic resonance imaging, Pediatr. Radiol. 48 (2018) 1945–1954, https://doi.org/10.1007/s00247-018-4235-4.

[18] K. Tanimura, M. Morizane, M. Deguchi, Y. Ebina, U. Tanaka, Y. Ueno, K. Kitajima, T. Maeda, K. Sugimura, H. Yamada, A novel scoring system for predicting adherent placenta in women with placenta previa, Placenta 64 (2018) 27–33, https://doi.org/10.1016/j.placenta.2018.02.005.

[19] Q. Li, H. Zhou, K. Zhou, J. He, Z. Shi, Z. Wang, Y. Dai, Y. Hu, Development and validation of a magnetic resonance imaging-based nomogram for predicting invasive forms of placental accreta spectrum disorders, J. Obstet. Gynaecol. Res. (2021), https://doi.org/10.1111/jog.14982.

[20] F.A. Pain, A. Dohan, G. Grange, L. Marcellin, J. Uzan-Augui, F. Goffinet, P. Soyer, V. Tsatsaris, Percreta score to differentiate between placenta accreta and placenta percreta with ultrasound and MR imaging, Acta Obstet. Gynecol. Scand. 101 (2022) 1135–1145, https://doi.org/10.1111/AOGS.14420.

[21] V. Romeo, C. Ricciardi, R. Cuocolo, A. Stanzione, F. Verde, L. Sarno, G. Improta, P. P. Mainenti, M. D'Armiento, A. Brunetti, S. Maurea, Machine learning analysis of MRI-derived texture features to predict placenta accreta spectrum in patients with placenta previa, Magn. Reson. Imaging 64 (2019), https://doi.org/10.1016/j.mri.2019.05.017.

[22] F. Verde, A. Stanzione, R. Cuocolo, V. Romeo, M. Di Stasi, L. Ugga, P.P. Mainenti, M. D'Armiento, L. Sarno, M. Guida, A. Brunetti, S. Maurea, Segmentation methods applied to MRI-derived radiomic analysis for the prediction of placenta accreta spectrum in patients with placenta previa, Abdom. Radiol. 1 (2023) 1–9, https://doi.org/10.1007/s00261-023-03963-5.

[23] N. Siauve, How and why should the radiologist look at the placenta? Eur. Radiol. 29 (2019) 6149–6151, https://doi.org/10.1007/s00330-019-06373-8.

[24] Y. Hu, W. Chen, C. Kong, G. Lin, X. Li, Z. Zhou, S. Shen, L. Chen, J. Zhou, H. Zhao, Z. Yu, Z. Wang, C. Lu, J. Ji, Prediction of placenta accreta spectrum with nomogram combining radiomic and clinical factors: A novel developed and validated integrative model, Int. J. Gynecol. Obstet. (2023), https://doi.org/10.1002/ijgo.14710.

[25] L. Peng, Z. Yang, J. Liu, Y. Liu, J. Huang, J. Chen, Y. Su, X. Zhang, T. Song, Prenatal Diagnosis of Placenta Accreta Spectrum Disorders: Deep Learning Radiomics of Pelvic <scp>MRI</scp>, J. Magn. Reson. Imaging (2023), https://doi.org/10.1002/jmri.28787.

[26] O.C.C. No, 7: Placenta Accreta Spectrum, Obstet. Gynecol. 132 (2018) E259–E275, https://doi.org/10.1097/AOG.0000000000002983.

[27] A. Zlotnik, V. Abraira, A general-purpose nomogram generator for predictive logistic regression models, Stata J. (2015).

[28] G. Hughes, Youden's index and the weight of evidence revisited, Methods, Inf. Med. 54 (2015) 576–577, https://doi.org/10.3414/ME15-04-0007.

[29] R.M. Silver, Abnormal Placentation, Obstet. Gynecol. 126 (2015) 654–668, https://doi.org/10.1097/AOG.0000000000001005.

[30] E. Jauniaux, J.C. Kingdom, R.M. Silver, A comparison of recent guidelines in the diagnosis and management of placenta accreta spectrum disorders, Best Pract. Res. Clin. Obstet. Gynaecol. 72 (2021) 102–116, https://doi.org/10.1016/j.bpobgyn.2020.06.007.

[31] S. Maurea, F. Verde, P.P. Mainenti, L. Barbuto, F. Iacobellis, V. Romeo, R. Liuzzi, G. Raia, G. De Dominicis, C. Santangelo, L. Romano, A. Brunetti, Qualitative evaluation of MR images for assessing placenta accreta spectrum disorders in patients with placenta previa: A pilot validation study, Eur. J. Radiol. (2022), https://doi.org/10.1016/j.ejrad.2021.110078.

[32] G. Capannolo, A. D'Amico, S. Alameddine, R. Di Girolamo, A. Khalil, G. Calì, I. T. Trish, C.M. Coutinho, M. Herrera, M. Liberati, A. Lucidi, J. Palacios-Jaraquemada, D. Buca, F. D'Antonio, Placenta accreta spectrum disorders clinical practice guidelines: A systematic review, J. Obstet. Gynecol. Res. 49 (2023) 1313–1321, https://doi.org/10.1111/jog.15544.

[33] F. D'Antonio, C. Iacovella, J. Palacios-Jaraquemada, C.H. Bruno, L. Manzoli, A. Bhide, Prenatal identification of invasive placentation using magnetic resonance imaging: systematic review and meta-analysis, Ultrasound Obstet. Gynecol. 44 (2014) 8–16, https://doi.org/10.1002/uog.13327.

[34] B.D. Einerson, C.E. Rodriguez, A.M. Kennedy, P.J. Woodward, M.A. Donnelly, R. M. Silver, Magnetic resonance imaging is often misleading when used as an adjunct to ultrasound in the management of placenta accreta spectrum disorders, Am. J. Obstet. Gynecol. 218 (618) (2018) e1–618.e7, https://doi.org/10.1016/j.ajog.2018.03.013.

[35] B.K. Dwyer, V. Belogolovkin, L. Tran, A. Rao, I. Carroll, R. Barth, U. Chitkara, Prenatal diagnosis of placenta accreta: Sonography or magnetic resonance imaging? J. Ultrasound Med. (2008) https://doi.org/10.7863/jum.2008.27.9.1275.

[36] M.A. Maher, A. Abdelaziz, M.F. Bazeed, Diagnostic accuracy of ultrasound and MRI in the prenatal diagnosis of placenta accreta, Acta Obstetricia et Gynecologica Scandinavica 92 (2013) 1017–1022, https://doi.org/10.1111/aogs.12187.

[37] K.E. Fitzpatrick, S. Sellers, P. Spark, J.J. Kurinczuk, P. Brocklehurst, M. Knight, Incidence and Risk Factors for Placenta Accreta/Increta/Percreta in the UK: A National Case-Control Study, PLoS One 7 (2012) e52893.

[38] C.V. Ananth, D.A. Savitz, E.R. Luther, Maternal Cigarette Smoking as a Risk Factor for Placental Abruption, Placenta Previa, and Uterine Bleeding in Pregnancy, Am. J. Epidemiol. 144 (1996) 881–889, https://doi.org/10.1093/oxfordjournals.aje.a009022.

[39] P. Taipale, M.-R. Orden, M. Berg, H. Manninen, I. Alafuzoff, Prenatal Diagnosis of Placenta Accreta and Percreta With Ultrasonography, Color Doppler, and Magnetic Resonance Imaging, Obstet. Gynecol. 104 (2004) 537–540, https://doi.org/10.1097/01.AOG.0000136482.69152.7d.

[40] J.I. Yang, Y.K. Lim, H.S. Kim, K.H. Chang, J.P. Lee, H.S. Ryu, Sonographic findings of placental lacunae and the prediction of adherent placenta in women with placenta previa totalis and prior Cesarean section, Ultrasound Obstet. Gynecol. 28 (2006) 178–182, https://doi.org/10.1002/uog.2797.

[41] W.C. Baughman, J.E. Corteville, R.R. Shah, Placenta Accreta: Spectrum of US and MR Imaging Findings, Radiographics 28 (2008) 1905–1916, https://doi.org/10.1148/rg.287085060.

[42] Y. Ueno, T. Maeda, U. Tanaka, K. Tanimura, K. Kitajima, Y. Suenaga, S. Takahashi, H. Yamada, K. Sugimura, Evaluation of interobserver variability and diagnostic performance of developed MRI-based radiological scoring system for invasive placenta previa, J. Magn. Reson. Imaging (2016), https://doi.org/10.1002/jmri.25184.

[43] A. Lax, M.R. Prince, K.W. Mennitt, J.R. Schwebach, N.E. Budorick, The value of specific MRI features in the evaluation of suspected placental invasion, Magn. Reson. Imaging 25 (2007) 87–93, https://doi.org/10.1016/j.mri.2006.10.007.

[44] A. Familiari, M. Liberati, P. Lim, G. Pagani, G. Cali, D. Buca, L. Manzoli, M. E. Flacco, G. Scambia, F. D'antonio, Diagnostic accuracy of magnetic resonance imaging in detecting the severity of abnormal invasive placenta: a systematic review and meta-analysis, Acta Obstet. Gynecol. Scand. 97 (2018) 507–520, https://doi.org/10.1111/aogs.13258.

[45] K.K. Patel-Lippmann, V.B. Planz, C.H. Phillips, J.M. Ohlendorf, L.C. Zuckerwise, M. Moshiri, Placenta Accreta Spectrum Disorders: Update and Pictorial Review of the SAR-ESUR Joint Consensus Statement for MRI, Radiographics 43 (2023) e220090.

[46] J.P. Zawaideh, S. Freeman, J. Smith, A. Bruining, T.J. Sadler, L. Carmisciano, H. C. Addley, Placental MRI: Identification of radiological features to predict placental attachment disease regardless of reader expertise, Eur. J. Radiol. 149 (2022), 110203, https://doi.org/10.1016/j.ejrad.2022.110203.

[47] L. Alamo, A. Anaye, J. Rey, A. Denys, G. Bongartz, S. Terraz, S. Artemisia, R. Meuli, S. Schmidt, Detection of suspected placental invasion by MRI: Do the results

depend on observer' experience? Eur. J. Radiol. 82 (2013) e51–e57, https://doi.org/10.1016/j.ejrad.2012.08.022.

[48] E. Jauniaux, L. Grønbeck, C. Bunce, J. Langhoff-Roos, S.L. Collins, Epidemiology of placenta previa accreta: a systematic review and meta-analysis, BMJ Open 9 (2019) e031193.

[49] P. Jha, L. Pōder, C. Bourgioti, N. Bharwani, S. Lewis, A. Kamath, S. Nougaret, P. Soyer, M. Weston, R.P. Castillo, A. Kido, R. Forstner, G. Masselli, Society of Abdominal Radiology (SAR) and European Society of Urogenital Radiology (ESUR) joint consensus statement for MR imaging of placenta accreta spectrum disorders, Eur. Radiol. 30 (2020) 2604–2615, https://doi.org/10.1007/s00330-019-06617-7.